View metadata, citation and similar papers at core.ac.uk

brought to you by CORE

provided by IntechOpen

We are IntechOpen, the world's leading publisher of Open Access books Built by scientists, for scientists

4,800
Open access books available

122,000
International authors and editors

135M
Downloads

Our authors are among the

154
Countries delivered to

TOP 1%
most cited scientists

12.2%
Contributors from top 500 universities

CLARIVATE ANALYTICS BOOK CITATION INDEX INDEXED

WEB OF SCIENCE™

Selection of our books indexed in the Book Citation Index in Web of Science™ Core Collection (BKCI)

Interested in publishing with us?
Contact book.department@intechopen.com

Numbers displayed above are based on latest data collected.
For more information visit www.intechopen.com

2

Optical Sensors Based on Opal Film and Silica Nanoparticles Modified with a Functional Dye

Ivan Boldov[1], Natalia Orlova[2], Irina Kargapolova[2], Alexandr Kuchyanov[1], Vladimir Shelkovnikov[2] and Alexandr Plekhanov[1]
[1]*Institute of Automation and Electrometry, Siberian Branch, Russian Academy of Sciences,*
[2]*Novosibirsk Institute of Organic Chemistry, Siberian Branch, Russian Academy of Sciences, Russia*

1. Introduction

Chemical sensing using optics is under extensive research all over the world and many optical chemical sensors are finding increasing application in industry, environmental monitoring, medicine, biomedicine and chemical analysis (Baldini et al., 2006). Optical sensors can be used as fiber optics microsensors, as planar coatings in bioreactors, in microtiterplate format, in disposable single-shot device, and as planar membranes that can be imaged using sensing camera. The spectral range extends from the UV to the infrared, and from absorption to emission and to surface plasmon resonance (Narayanaswamy & Wolfbeis, 2004). Hence, a variety of schemes are conceivable. The purpose of this chapter is to introduce the concept of highly sensitive and selective optical sensors for different type reagent based on opal film and silica nanoparticles modified with a functional dye.

In the last two decades photonic crystals have much potential for creation of new optical functional materials (Joannopoulos et al., 2008). Photonic crystals are inhomogeneous media with a periodically varying relative permittivity. The capability of such periodic structures to form photonic band gaps changes the paradigm of controlling the propagation of light. For this reason, the features of the behavior of refracted light in the allowed bands and at the edge of the band gaps currently attract a lot of attention. A number of unusual properties of the propagation of light in photonic crystals such as the refraction of light in negative media (Foteinopoulou et al., 2003) and the effect of a superprism and the self-collimation of light (Kosaka et al., 1998) were recently revealed. It was proposed to use these effects for creating a supersensitive light beam splitter (Baba & Nakamura, 2002; Wu et al., 2003) and for controlling an optical flux (Chen et al., 2004). Moreover, schemes with photonic crystals can underlie supersensitive optical chemical sensors (Yakimansky et al., 2009). For such applications, it is important to determine and analyze regions with a strong angular dispersion in optical systems with photonic crystals and to study the behavior of light at the interface of photonic crystals with other optical media. Extension of sensory capabilities of photonic crystals by the chemical modification of silica nanoparticles with functional dyes offers promise as a high selective fluorescent sensor and many ways to miniaturize and integrate photonic devices on high functionality optical chips.

We show state-of-the-art fabrication of photonic crystals in the visible optical region based on a single-crystal opal platform (Plekhanov et al., 2006). We have investigated a new effect appearing in the displacement of the photonic bang gap on the background of the spectrum of backward diffracted and reflected Bragg waves at the grazing incident of white-light beam on the glass – photonic crystal opal film interface. The physical basis for observable effect is such characteristics of the photonic crystals as a strong angular dispersion and the dependence of the spectral position of photonic bang gap on the amount and type of analyte. It was found that the spectrum of the Bragg backward reflection and refraction manifested the photonic bang gap, which changes its position under insignificant change of the concentration of vapor of a range of substances (isopropyl alcohol, dibutylamin, tributylamine, water, ammonia), filling the photonic crystal. We consider this effect in second part of the chapter.

Quick analysis of the presence of a particular analyte is a fairly common task. In this case, as a rule do not need ultra-high sensitivity and reversibility. The implementation of spectroscopic schemes into a useful sensing scheme has been hampered though, by the lack of appropriate materials including silica nanoparticles with functional organic dyes. This chapter will also address the progress made in the past years. We have developed the method for the chemical modification of silica nanoparticles with a pyrylium dye under the sol–gel synthesis conditions. The films of silica particles modified with a pyrylium dye gave luminescence in visible spectral range upon treatment with a solution of butylamine.

During the last 15 years, fiber optics sensors have been developed and evaluated to assess air, water and soil contamination level. These sensors utilize the optical properties of chemicals or products of chemicals or biological reactions to assess contaminants to monitor process quality, provide compliance monitoring and evaluate real-time insitu contaminant levels in uncontrolled and remediated hazardous waste sites. The coating of the thin-film nanostructures based on silica nanoparticles on the surface of optical fiber allows significantly extend the scope of fiber-optic sensors (Boldov et al., 2011). We have realized for the first time a fiber-optic chemical sensor for butylamine.

2. Features of the manifestation of a stop band in the spectrum of light diffracted at a glass–opal interface

In this section, we report the results of the investigation of a new effect of the displacement of the photonic band gap (stop band) against the unchanged spectrum of diffracted white light at the glass–thin opal film interface and the possibilities of using this effect to create optical chemical sensors and to control spectral light fluxes (Plekhanov et al., 2009).

Artificial opal films consisting of spherical silicon dioxide nanoparticles were used as photonic crystals in the experiments. The experiments were performed with monolayer and multilayer films and heterostructures consisting of several types of layers with various sphere diameters from 220 to 280 nm. Photonic crystal films were grown by the movable meniscus method from the suspension of monodisperse spherical particles of SiO_2 on glass prisms; these samples allow for the investigation of the spectra for all of the angles of incidence of light on the glass–photonic crystal interface. The moving meniscus method makes it possible to grow photonic crystals with the structure ordered over the entire area. In addition, monolayer opal films, which had a domain structure, were deposited by the method of the short-term immersion of a prism into a suspension.

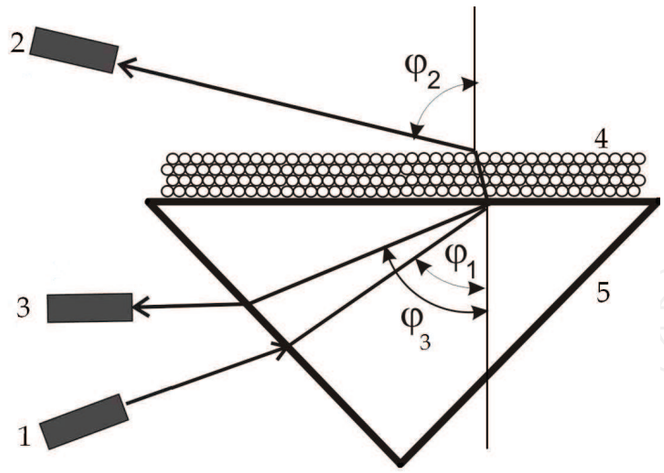

Fig. 1. Scheme of the interaction of light with the opal film photonic crystal on the glass substrate: 1 – halogen lamp; 2, 3 - spectrometer; 4 – photonic crystal film; 5 – glass substrate.

A white-light beam from a halogen lamp was incident on a face of a glass prism and, then, on the glass–photonic crystal interface (see the interaction scheme in Fig. 1.). Here, we consider refracted and reflected Bragg waves for which the directions of tangential projections of wave vectors are opposite to the corresponding projection of the wave vector of the incident wave. Refracted (2) and backward reflected (3) waves were observed after the incidence of the white-light beam (1) from the glass with the reflective index n_g = 1.51 at the interface between this medium and the three-dimensional photonic crystal film deposited on its surface. The angles φ_1 and φ_3 are measured in the glass and the angle φ_2 is measured in the air between the normal vector to the growth plane of the photonic crystal and the wave propagation direction. The angular dependences of the spectra of these waves were detected by an «Avantes» spectrometer whose optical fiber receiver was mounted on the arm of a goniometer. The angular resolution was $\Delta\varphi \approx 1°$.

The dispersion of light was examined for various synthesized photonic crystals at various angles of incidence φ_1 of white light on the (glass–photonic crystal) interface. The effect of the strong angular dispersion $\varphi_{2,3}(\lambda)$ in refracted light and light reflected back to the glass was observed for the angles of incidence φ_1 of white light larger than ≈ 41.5 , i.e., under the condition of the total internal reflection at the (photonic crystal–air) interface. For this reason, the observation of this dispersion is impossible at the incidence of light on the photonic crystal from air. Figure 2 shows the angles φ_2 and φ_3 of Bragg waves refracted and reflected from the (glass–photonic crystal) interface, respectively, as functions of the wavelength λ at φ_1 = 51.

The maximum angular dispersion, i.e., the maximum derivative $\partial\varphi_{2,3}(\lambda)/\partial\lambda$, is observed in the wavelength range λ = 580–590 nm for the opal monolayer. It is apparently caused by a strong change in the curvature of the isoenergetic surface (Kosaka et al., 1998), the normal vector to which determines the direction of the group velocity of the light wave with a given wavelength. The investigation of the photonic crystal samples containing two to hundreds of opal layers shows a number of qualitative differences. Even for several opal layers for the refracted and reflected waves, the monotonic dependence $\varphi_{2,3}(\lambda)$ was observed in a wide wavelength range and for reflection angles up to $\varphi_3 \approx 12°$. As the number of opal ball layers

increases, the intensity of refracted and reflected light increases in the directions satisfying the Bragg condition. Moreover, with an increase in the number of the layers, a dip and a peak appear in the spectra of the waves passed through the photonic crystal and reflected from it at the wavelength coinciding with the position of the stop band of the photonic crystal. For the photonic crystal heterostructures consisting of two types of layers with different diameters of the balls, two spectral features corresponding to the stop bands of different photonic crystal layers appear in the spectrum of the waves.

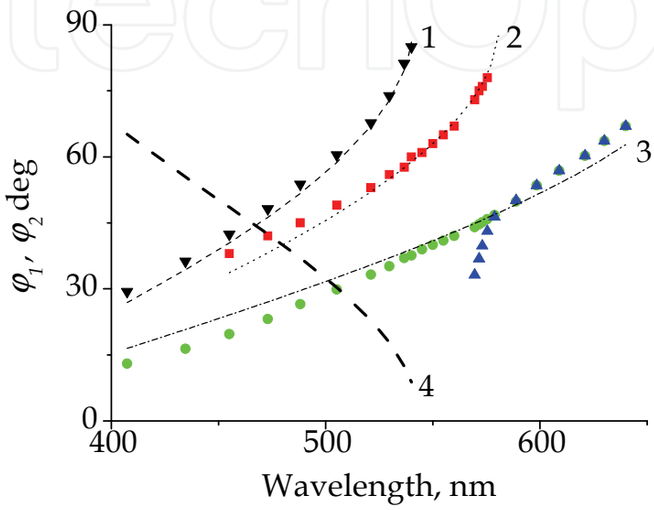

Fig. 2. Angles of refraction, φ_2, and reflection, φ_3, of Bragg waves at the (glass–photonic crystal) interface versus the wavelength λ at the angle of incidence of white light $\varphi_1 = 51°$ for the (▲) reflection in the case of the opal monolayer, (●) reflection in the case of the photonic crystal, (■) refraction in the case of the opal monolayer, and (▼) refraction in the case of the photonic crystal. The solid curve is the position of the stop band of the photonic crystal calculated by Eq. (2). The dashed (1), dotted (2), and dash–dotted (3) curves are the approximation by Eq. (1) with $n_{eff} = 1.36$, 1.11, and 1.51, respectively.

It was revealed that the spectra of reflected and refracted Bragg waves have third order azimuthally anisotropy and were observed only for the three directions of the incident beams, $[\bar{2}11]$, $[11\bar{2}]$ and $[1\bar{2}1]$, lying in the (111) plane (the notation refers to a face-centered cubic lattice). A comparison shows that the light scattering spectra from the photonic crystals obtained by different methods mentioned above are similar to each other, but anisotropy was not observed in the case of the photonic crystal with the domain structure formed in the immersion method. This indicates that the spatial anisotropy of the effect is attributed to the hexagonal structure of the photonic crystal in the (111) plane and is responsible for the unchanged angular dispersion of white light.

The scattering of light at the glass–photonic crystal interface is described by the Bragg diffraction equation following from the condition that the tangential component of the wave vector of the incident wave is equal to the sum of the tangential components of the wave vector of the refracted wave and the corresponding vector of the crystal lattice. For the first unit cell of the photonic crystal, this equation has the following form and describes the angular dispersion:

$$\varphi_3(\lambda) = \arcsin\left(\frac{\lambda/a - n_g \sin\varphi_1}{n_{eff}}\right), \quad (1)$$

where φ_1 and φ_3 are the angles of incidence and reflection of the light wave, respectively; λ is the light wavelength in vacuum; n_g and n_{eff} are the refractive indices in the homogeneous and periodic media, respectively; and a is the lattice period in the direction of the incidence of light. The angular dispersion $\varphi_2(\lambda)$ for the refracted light is described by Equation (1) with the change $\varphi_3 \rightarrow \varphi_2$ and Snell's law for the passage of light from the photonic crystal to air.

The curves calculated by Equation (1) well approximate the experimental data. The dash–dotted curve (3) (Fig. 2.) is the approximation by Equation (1) for the Bragg wave reflected from the opal monolayer with $n_{eff} = n_g = 1.51$ (because the incident and reflected waves propagate in glass). The dotted curve (2) (Fig. 2.) is the approximation for the refracted Bragg wave with $n_{eff} = 1.11$ (this n_{eff} value is taken for the boundary layer (Kalinin et al., 2006). For the multilayer opal film with the number of layers beginning with two, the spectral dependence $\varphi_2(\lambda)$ is also described by Equation (1), but with the refractive index of the photonic crystal $n_{eff} = 1.36$ (the dashed curve (1) in Fig. 2.). The calculations were performed taking into account the refraction of reflected light at the glass–photonic crystal interface and the electron microscopy data from which the nanoparticle size was determined as $D = 254$ nm.

The most important property of the optical scheme under consideration is the manifestation of the properties of the photonic crystals and diffraction at the glass–photonic crystal interface. The experiments show that the introduction of a CCl_4 immersion liquid, which has a refractive index close to the value for quartz, to the photonic crystal does not shift the spectrum of Bragg waves; i.e., the angular dependence of the spectrum of the halogen lamp is almost insensitive to the refractive index of the photonic crystal. For this reason, this spectrum is used as a reference against which the spectral position of the stop band of the photonic crystal is measured.

The curve 2 in Fig. 3. shows the spectrum of the refracted Bragg wave. The stop band of the photonic crystal is observed in this spectrum as a dip. The position of the stop band is determined by jointly solving Equation (1) and the equation determining the behavior of the stop band when light is incident from air on the photonic crystal film at the angle $\varphi = -\varphi_2$:

$$\lambda = \sqrt{\frac{8}{3}} D n_{eff} \cos(\varphi). \quad (2)$$

The position of the stop band of the photonic crystal extracted from our experimental data is in good agreement with that calculated by Equation (2). The solid curve (4) in Fig. 2. corresponds the position $\lambda(\varphi)$ of the stop band of the photonic crystal that has the effective refractive index $n_{eff} = 1.36$ and consists of SiO_2 balls with $D = 254$ nm. The point of the intersection of this curve with the experimental dependence $\varphi_2(\lambda)$ for the wave refracted in the photonic crystal corresponds to the angle φ_2 at which the pronounced dip is seen in the spectrum of the refracted wave (see Fig. 3.).

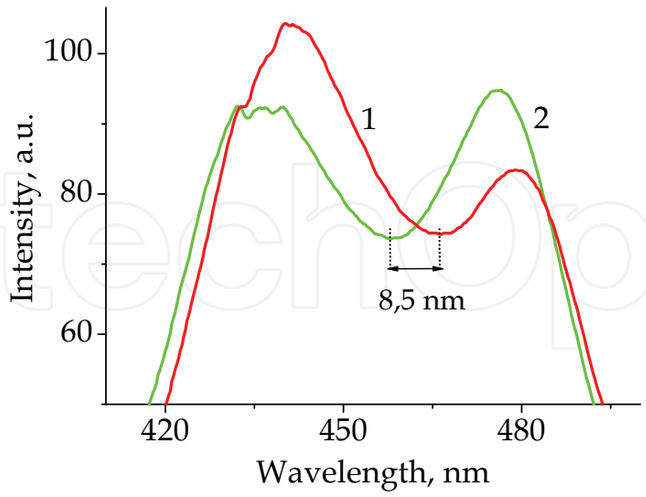

Fig. 3. Spectrum of the refracted Bragg wave with the stop band (curve 2) before and (curve 1) after the action of ammonia vapors with a density of 0.2 mg/m^3.

We found that the position of the stop band in the unchanged spectrum of reflected and refracted Bragg waves for light incident from glass on the interface with the photonic crystal is highly sensitive to a small change in the concentration of vapors of water, ammonia, ethanol, or isopropyl alcohol. The observed effect is reversible and can be used to create optical chemical sensors.

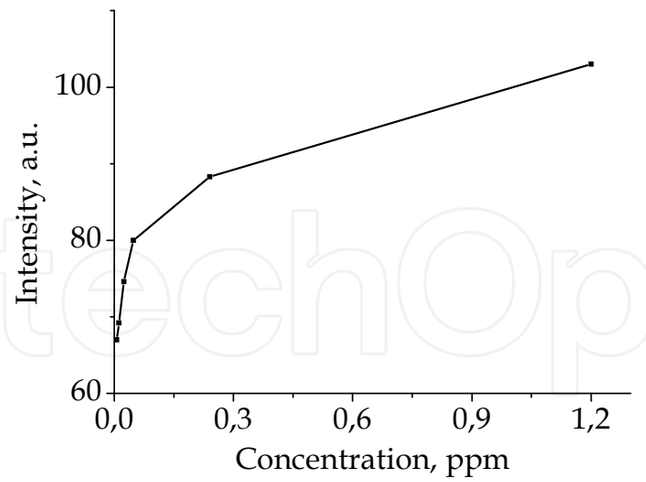

Fig. 4. Effect of ammonia concentration on the intensity of the reflected Bragg wave.

The variation in analyte concentration is measured by the signal from the photodiode (position 3 in Fig. 1.). The photodiode was located so that it recorded the signals in the wing of stop band. In this case the signal from the photodiode was proportional to the change in concentration of the analyte. At certain angles of observation we have observed a maximum in the spectrum of the reflected wave associated with the presence of the stop band. The

intensity of reflected light is several times higher than refractive one, so the implementation of an optical chemical sensor in this geometry is preferable. In this case a functional diagram of the sensor contains two photodiodes measuring the intensity of long- and short-wavelength wings of Bragg maximum. The maximum are shifted in wavelength with a change of analyte concentration. It leads to an increase in a signal of a photodiode and a decrease in another. Electric circuit comparing the signals from the photodiodes allows to significantly increase the sensitivity of registration and to exclude fluctuations in the intensity halogen lamp. Figure 4 shows the effect of ammonia concentration on the intensity of the reflected Bragg wave.

It is well known that siloxane (Si–O–Si) and silanol (Si–OH) groups are present on the surface of silica nanoparticles. Their extremal density can reach five OH groups per nanometer squared. The presence of a mobile hydrogen atom in polar hydroxyl groups gives rise to the effective interaction with the molecules of the gas and liquid phases by two ways. The first interaction is electrostatic attraction between hydroxyl groups on the silica surface and the surrounding dipole molecules. In addition, hydrogen bonds can appear between hydroxyl groups and the surrounding molecules if these molecules have an undivided electron pair. For this reason, water and ammonia, being the most polar molecules among those listed above, manifest the strongest electrostatic interaction and form the strongest hydrogen bonds with the silica surface with a high probability of the formation of monolayers or cluster island films on the surface of nanoparticles. Ethanol and isopropyl alcohol also form hydrogen bonds owing to the presence of an oxygen atom and a mobile hydrogen atom, but these bonds are weaker than those formed by water or ammonia, because the polarity of alcohols is smaller. Nonpolar carbon tetrachloride molecules, which do not have atoms capable of forming hydrogen bonds, almost do not interact with the silica surface.

Indeed, the experiments show that the maximum spectral shift ≈8 nm of the stop band of the photonic crystal is observed under the action of water or ammonia vapors. Figure 3 shows the spectra of the refracted Bragg waves for the photonic crystal in air without (curve 2) and with (curve 1) ammonia vapors with an NH_3 density of about 0.2 mg/m^3 . The data were obtained at the angle of incidence of light φ_1 = 51°. The estimates show that the ammonia molecular monolayer uniformly covering the surface of the opal balls gives rise to a change in n_{eff} in ammonia vapors by $\Delta n_{eff} \approx 0.004$, which corresponds to the spectral shift of the center of the stop band by about 1 nm. However, it should be taken into account that silica balls can consist of globules (Baryshev et al., 2007) and their specific surface can be larger by an order of magnitude, which was not taken into account in the estimates.

A smaller spectral shift of 1–2 nm was observed for ethanol and isopropyl alcohol vapors and was absent for carbon tetrachloride vapors; this observation corresponds to a decreasing sequence of the dipole moments of these molecules. The revealed selectivity can be enhanced by the controlled chemical modification of the surface of silica nanoparticles as a carrier. For example, the amount of absorbed water is determined by the type of the functional group and decreases in the series SO_3H > $N(CH_3)_3Cl$ > NH_2 > OH (Sakai et al., 1989). By fixing more specific complex organic molecules on the surface (Orlova et al., 2009), it is possible to significantly expand the functionality of a sensor based on the described effect, when the interaction of selective functional groups on the surface of an element with an identified element gives rise to its adsorption and results in a change in the number of the physical parameters of the modified photonic crystals.

3. The synthesis and physical-chemical properties of silica nanoparticles modified with pyrylocyanine dye

The luminescence properties of organic dyes are enhanced in the mesoporous nanostructures of silica and the light resistance of these dyes increases (Collinson, 2002; Sokolov et al., 2007). Thus, the binding of luminescent functional dyes with silica nanoparticles is promising for the use of modified silica nanoparticles as luminescence sensors. We have developed a method for the preparation of solid sensors for amine-type reagents based on luminescent silica nanoparticles modified with a functional pyrylocyanine dye.

It is known that pyrylocyanine dyes interact with primary amines to form pyrydocyanines (Balaban et al., 1982). Pyrydocyanines exhibit luminescence, which is different from the luminescence of the starting pyrylocyanines; this can be used for the luminescence detection of organic amines (Höfelschweiger, 2005).

3.1 The synthesis of silica nanoparticles modified with pyrylocyanine dye

The method of modified nanoparticles formation includes three steps.

The first step is a synthesis of an oligomer precursor containing trimethoxysilyl groups and a pyrylium dye. The covalent bond between the dye and the nanoparticle occurred through a precursor, which was obtained by the copolymerization of an oxiranyl derivative of alkoxysilane and a dye containing the oxirane group. A pyrylocyanine dye capable of covalently binding to the skeleton of a silica nanoparticle was synthesized for the modification of silica nanoparticles. The oxirane group was introduced into the aldehyde moiety of the dye molecule (Liang et al., 2002).

To avoid premature epoxide ring opening, we proposed a reaction scheme for the functionalization of nanoparticles, which involved the initial reaction of aldehyde **2** with an epoxy derivative of trialkoxysilane. The epoxide ring opening reaction in aldehyde **2** in the presence of trimethoxy-[2-(7-oxabicyclo-[4.1.0]hept-3-yl)-ethyl]-silane **5** was performed with the addition of a $BF_3 \cdot Et_2O$ (boron trifluoride etherate) catalyst. As a result, precursor **6** was formed; because of the presence of an aldehyde group, this precursor retained its ability to undergo subsequent condensation with 2,4,6-trimethylpyrylium perchlorate **3** (Fig. 5.) to give precursor **7.**

The second step is a silica clusters preparation.

The silicate sol was obtained by hydrolysis and condensation of tetraetoxysilane $Si(OEt)_4$. The process is shown on Fig. 6. The first stage is the hydrolysis catalyzed by the acid. The second stage is the condensation. The stages are alternate to form -Si-O-Si- containing clusters and further nanoparticles.

The third step is preparation of silica particles modified with pyrylocyanine dye.

Oligomer precursor **7** was introduced into a reaction with a hydrolyzed tetraethoxysilane sol. The resulting colloid solution was centrifuged, and the solvent was decanted. The precipitate was washed with acetonitrile to remove free dye; ethanol was added, and the precipitate was repeatedly dispersed to a colloid solution on a «Bandelin» ultrasonic homogenizer. As a result, a colloid solution of silica nanoparticles modified with pyrylocyanine **4** was obtained.

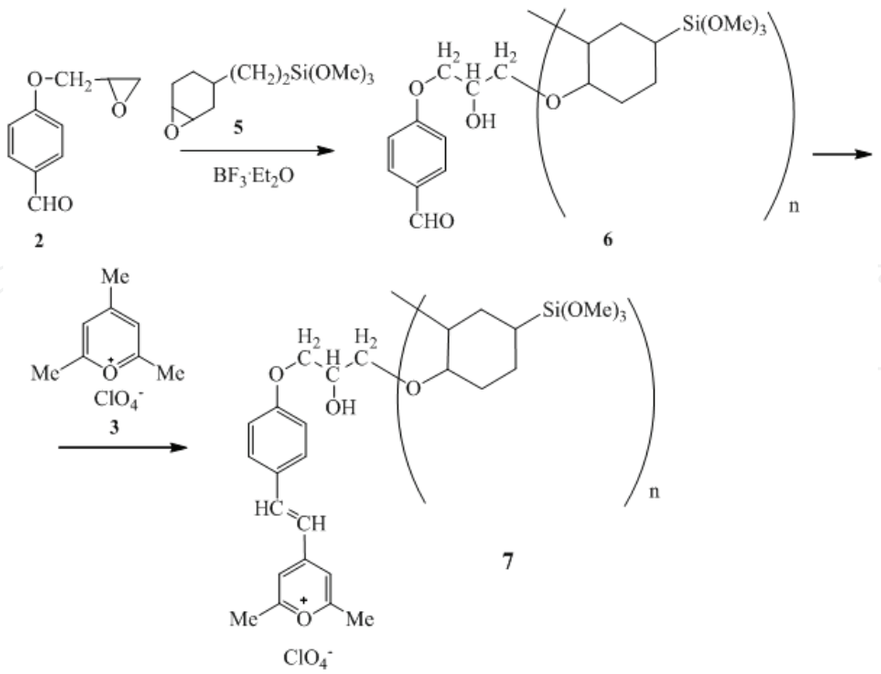

Fig. 5. The synthesis of an oligomer precursor containing trimethoxysilyl groups and a pyrylium dye.

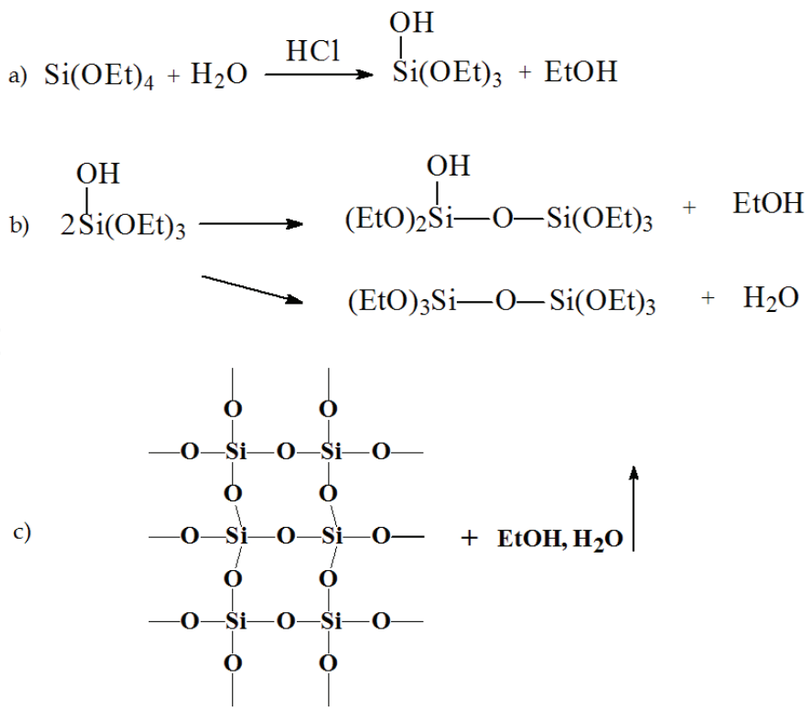

Fig. 6. The silica clusters preparation: (a) the hydrolysis catalyzed by the acid; (b) the condensation; (c) the alternating -Si-O-Si- containing clusters and further nanoparticles.

The resulting compounds were characterized by NMR, IR, and UV spectroscopy and spectrofluorometry. The NMR spectra were measured on an AC-200 instrument (Bruker), and the IR spectra were measured on a Vector 22 instrument (Bruker). The UV spectra were recorded on an 8453 spectrophotometer (Hewlett-Packard), whereas the fluorescence spectra were measured on a Cary Eclipse fluorimeter (Varian). The films of nanoparticles were studied by luminescence confocal microscopy on an LCM 750 microscope (Carl Zeiss) and by electron microscopy on a TM-1000 microscope (Hitachi).

To prepare films, the colloid solution of modified silica nanoparticles was supported onto a glass substrate by casting, washed with water and dried in air. An inhomogeneous opaque light orange film was formed.

3.2 The physical-chemical properties of silica nanoparticles modified with pyrylocyanine dye

Depending on the molar ratio between an aromatic aldehyde and a silicon-containing oxirane introduced into the reaction, different numbers of aldehyde and trimethoxysilyl groups were formed in precursor **6**. Based on the calculation of the relative signal intensities of these groups in the ^{1}H NMR spectra of copolymer **6**, we found that the number of reacted aldehyde molecules correlated with the initial oxirane : aldehyde ratio (see the Table 1.). Depending on the initial oxirane: aldehyde ratio, the precursor contained from 8 to 50 methoxysiliyl groups covalently bound to an aldehyde molecule.

Aldehyde amount dissolved in 1 ml of oxirane, g	Oxirane : aldehyde molar ratio	$(MeO)_2Si : H_{ald}$ integral intensity ratio
0.05	15 : 1	50 : 1
0.1	7.5 : 1	35 : 1
0.2	3.75 : 1	8 : 1

Table 1. Oxirane: aldehyde rations in copolymer 6, as found from the ^{1}H NMR spectra.

To determine the degree of modification of the resulting silica nanoparticles with pyrylocyanine **4**, we calculated the number of SiO structural units per dye molecule. The calculation was performed based on the ratio between the average molecular weight of a colored nanoparticle, which was obtained from absorbance data in the absorption spectra of a colloid solution

$$M_w = \frac{l\varepsilon[C]}{D}, \tag{3}$$

where [C] is the substance concentrationin g/l, and the molecular weight of the dye taken the same molar absorption coefficients of the dye in both species. As a result, we found that on average a dye molecule accounted for 48 SiO structural units.

3.2.1 Luminescent properties of the resulting modified silica particles

The luminescence response of a sensor based on silica nanoparticles modified with pyrylocyanine depends on the reaction of the dye with primary amines to result in luminescent pyrydocyanines. Therefore, we performed a reaction with a 10% solution of butylamine in ethanol on the modified colloid particles in solution and in a film. After the addition of 0.2 ml of the butylamine solution to 10 ml of a colloid solution of modified silica

particles, blue fluorescence was observed under UV illumination. Figure 7 shows the spectrum of this fluorescence. A portion of a film of silica nanoparticles modified with pyrylocyanine **4** on a glass substrate was treated with a butylamine solution, and the other portion of the film remained untreated.

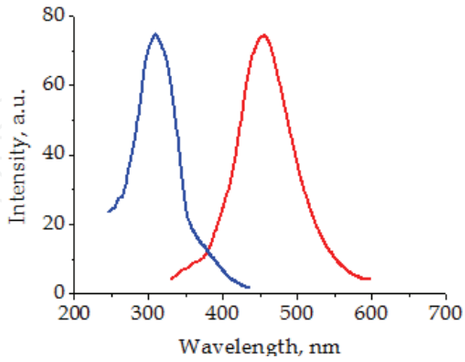

Fig. 7. Excitation (1) and luminescence (2) spectra of the reaction product of colloid particles modified with pyrylocyanines 4 with butylamine in ethanol.

Figure 8 shows the luminescence photographs obtained on a confocal microscope and the luminescence spectra of individual microregions in the untreated and treated films. The luminescence of nanoparticles modified with pyrylocyanine **4** exhibited a maximum at 600 nm; it changed to the luminescence of a pyrydocyanine dye with a maximum at 490 nm after treatment with butylamine.

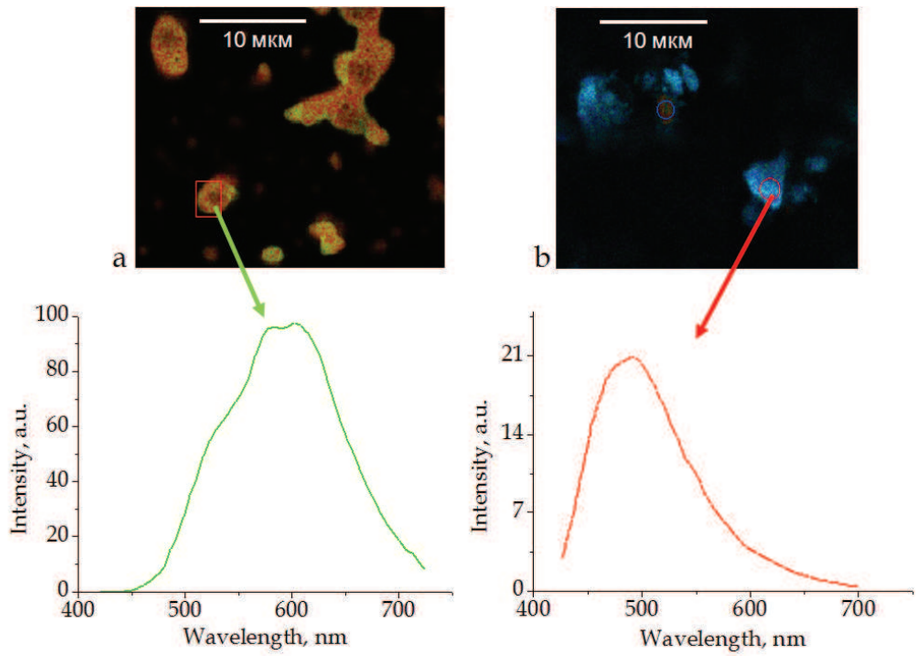

Fig. 8. Luminescence photographs and luminescent spectra of individual microregions of (a) an untreated film and (b) a film of silica nanoparticles modified with pyrylocyanine **4** treated with a 10% solution of butylamine in ethanol obtained on an LCM 750 confocal microscope upon laser excitation at a wavelength of 407 nm.

From a comparison of the luminescence spectra of a pyrydocyanine dye bound to silica nanoparticles in a film and the luminescence spectrum of this dye in a colloid solution, it follows (cf. Figs. 7 and 8) that, in the film, the luminescence spectra of the pyrydocyanine dye were broadened and shifted to the long-wavelength region, as compared with those of the colloid solution. The light resistance of silica particles modified with pyrylocyanine dye **4** in both a colloid solution and a film was studied under irradiation with monochromatic light at an intensity of 0.8 mW/cm^2 at a dye absorption maximum. The light source was a DKSSh-1000 lamp with an MDR-2 monochromator. No spectral changes occurred upon exposing the dye-modified nanoparticles both in a colloid solution and in a film at total exposures of 0.5–1 J/cm^2.

3.2.2 Change in film morphology upon amine treatment

The treatment of a nanostructured film of silica particles modified with a pyrylium dye with a solution of butylamine resulted in a change in the film morphology. Figures 9a and 9b show the micrographs, which were obtained on a Hitachi TM-1000 electron microscope, of a film of silica nanoparticles modified with pyrylocyanine **4** before and after treatment with a solution of butylamine, respectively. As can be seen in these micrographs, the treatment with a solution of butylamine resulted in a partial agglomeration of the initial loose nanostructured film to form spherical structures of micrometer sizes. In this case, it can be seen that some incompletely formed spherical microstructures were also structured at the nanolevel.

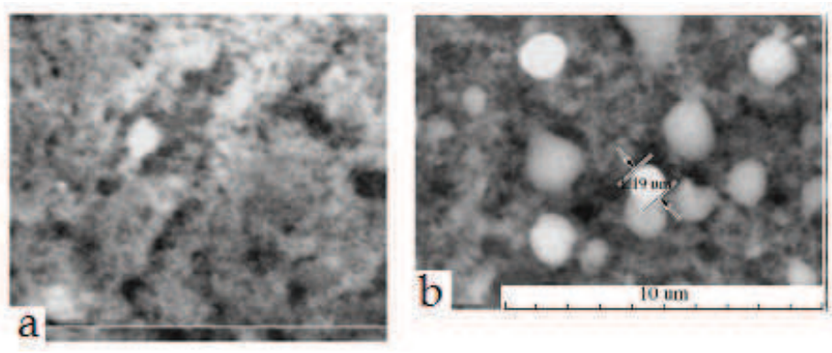

Fig. 9. Electron micrographs of a film obtained from a colloid solution of silica nanoparticles modified with dye 4 on a magnification of 10000X (a) before and (b) after treatment with butylamine.

4. Fiber-optic sensor for butylamine based on modified silica nanoparticles

Fiber optics is one of the most dynamically developing field of physics. The application of fiber optics in a range of sensors has several important advantages. Insensitivity to electromagnetic and radiation interference, chemical and thermal stability, remote sensing, relatively low cost makes these types of sensors indispensable in some cases. The coating of the thin-film nanostructures based on silica nanoparticles on the surface of optical fiber allows significantly extend the scope of fiber-optic sensors (Janotta et al., 2003; Xiao et al., 2005; Yan et al., 2009) It is known that amines are usually toxic and in some cases are strong carcinogens. One of the significant shortcomings of existing chemical sensors for amine-type compounds is the lack of selectivity. This chapter reports the results of experimental studies of selective sensor for butylamine based on nanostructure thin-film coated at the end of an

optical fiber. This film consists of silica nanoparticles of 8-10 nm modified with polymethine dyes. Pyrydocyanines exhibit luminescence, which is different from the luminescence of the starting pyrylocyanines. This effect was inventive incentive for the synthesis of pyrylocyanine **2** and pyrylocyanine **3** dyes, which selectively react with butylamine. Therefore, the binding of luminescent functional dyes with silica nanoparticles is promising for the use of optical chemical sensors. The pyrylocyanine dye have a covalent bond with the skeleton of silica nanoparticles. The method of chemical modification of silica nanoparticles in a sol-gel synthesis is described in (Orlova et al., 2009).

«Avantes AvaSpec-2048TEC» spectrometer with a spectral resolution of 1 nm was used in the studies of luminescence properties of the thin films, which are consist of modified silica nanoparticles. «Newport LQC 405 - 85E» semiconductor laser was used as a source of exciting light with a wavelength of 407 nm (Fig. 10.). The thin-film nanostructure is deposited on the end of a freshly cleaved optical fiber with a diameter of 600 μm by dropping into the solution of modified silica nanoparticles or deposition and subsequent drying a drop of the solution at the end of the fiber. We have experimentally found that the film of modified silica nanoparticles is durable to the various kinds of mechanical effects and demonstrates a high radiation resistance.

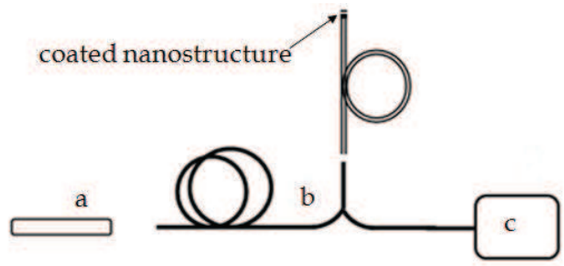

Fig. 10. Optical scheme of measuring; a – semiconductor laser, b - reflection probe, c – spectrometer.

A typical luminescence spectrum of the silica nanoparticles film modified with pyrylocyanine **3** dye has a pronounced peak at 660 nm. The film gives a green-yellow luminescence with a maximum at 560 nm after a treatment with 10% solution of butylamine (Fig. 11.).

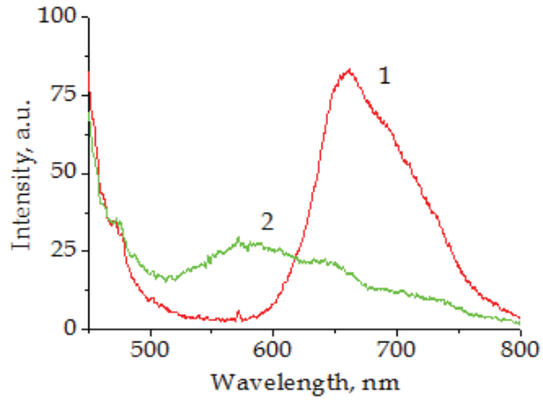

Fig. 11. Luminescence spectrum of the modified silica nanoparticles thin-film with pyrylocyanine **3** before (1) and after (2) treatment with butylamine solution.

It should be noted that the luminescence effect of the modified silica nanoparticles film after the treatment with other amino liquids leads only to the quenching of luminescence in the red spectrum, while the yellow-green luminescence does not appear. The minimum concentration of butylamine in ethanol was 10^{-3} mol/l in which possible to record the luminescent responses from the silica nanoparticles film modified with pyrylocyanine **3** dye.

In contrast to the silica nanoparticles film modified with pyrylocyanine **3** dye, the films modified with pyrylocyanine **2** do not have the luminescence before the treatment. The maximum of luminescence at 580 nm was exhibited after treatment with butylamine solution. On exposure to other amino substances, the luminescence peak does not appear which also shows selectivity for the analyte. To increase the amplitude of the luminescence response from the modified silica nanoparticles film coated on the end of optical fiber as a porous selective mirror was applied. The mirror is an artificial opal photonic-crystal film. The maximum of reflection of this mirror coincides with the peak of pyrylocyanine luminescence in modified silica nanoparticles after the treatment with butylamine solution.

It was achieved by choosing the diameter of monodisperse silica spheres of about 260 nm. The porosity of photonic crystal film allows butylamine and other substances easily penetrate into the modified silica nanoparticles film. The photonic crystal opal film was grown by moving meniscus method on the end of the optical fiber (Kalinin et al., 2006). For this purpose optical fiber is fixed in the suspension of monodisperse silica spheres on the surface under an angle of 15 degrees. The reflection spectrum of «photonic crystal mirror» deposited on the end of the optical fiber is practically coincided with the luminescence band of pyrylocyanine **2** dye in the region of 580 nm.

The experiments have demonstrated that the coating of the «photonic crystal mirrors» on the modified silica nanoparticles film leads to an increase in the amplitude of the reflected signal in 3 - 4 times (Fig. 12.). The photonic crystal film was a highly ordered hexagonal close-packed structure of the monodisperse silica spheres, and the crystallographic direction (111) was normal to the surface. The presence of «photonic crystal mirror» does not affect the rate of change of the optical response of sensory film.

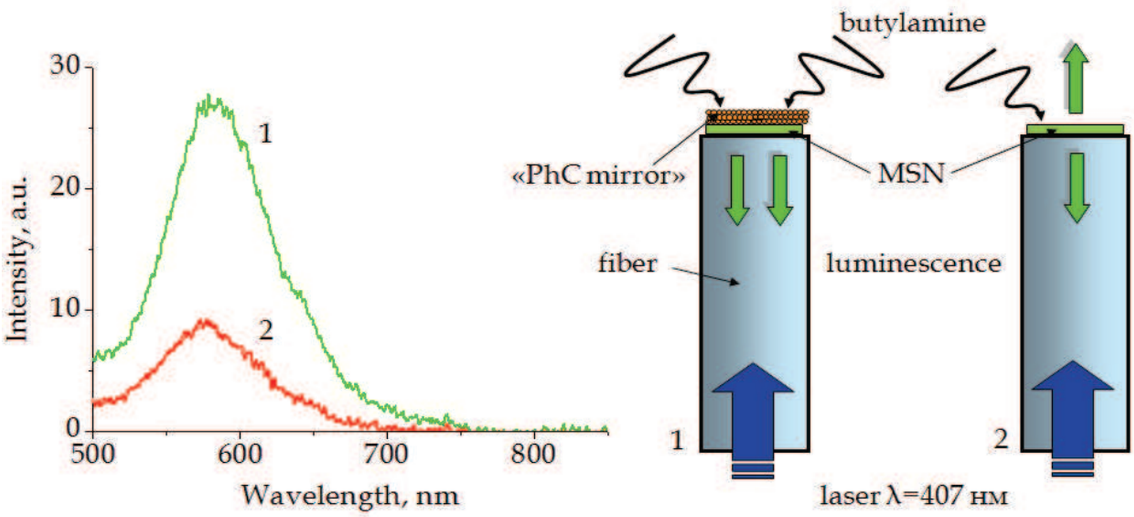

Fig. 12. Luminescence spectrum of modified silica nanoparticles with pyrylocyanine **2** with (1) and without (2) «photonic crystal mirror».

The further increase in the amplitude of a luminescence of modified silica nanoparticles might be enhanced due to the presence of nearby metallic nanoparticles such as Ag or Au (Geddes et al., 2003). We have found that the addition of Ag nanoparticles with a diameter of 5 - 7 nm into the modified silica nanoparticles film leads to an increase the luminescence in 2 - 3 times (see Fig. 13.).

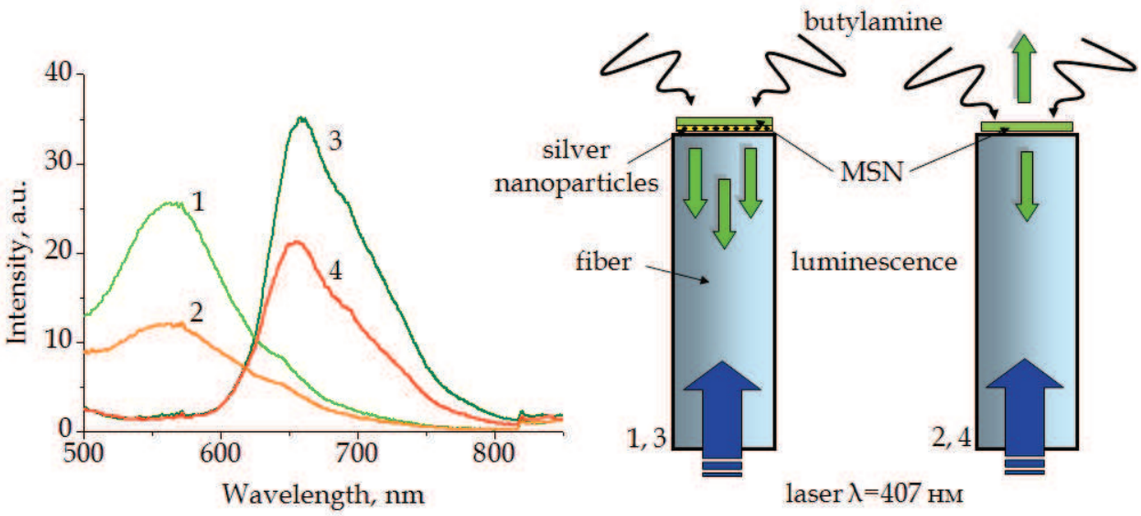

Fig. 13. Luminescence spectrum of modified silica nanoparticles with pyrylocyanine 3 before (3,4) and after (1,2) treatment with butylamine solution; with (1,3) and without (2,4) injection of silver nanoparticles.

5. Conclusion

This chapter proposed concept of highly sensitive and selective optical sensors for different type reagent based on negative light diffraction and refraction at a glass-opal interface and modified silica nanoparticles. The optical fiber butylamine chemical sensor based on selectively altering the luminescent properties of modified silica nanoparticles thin-film. The sensor component is a modified silica nanoparticles covalently bound with pyrylocyanine dye and deposited at the end of the optical fiber. A method for the chemical modification of silica nanoparticles with a pyrylium dye under sol–gel synthesis conditions was developed. The films of silica particles modified with a pyrylium dye were obtained; these films emitted luminescence in visible range of spectra. Upon the treatment of the films with a solution of butylamine, a fluorophore from the pyrydocyanine series was formed on the modified silica nanoparticles; this fluorophore emitted luminescence shifted in shortwave range of spectra. The film samples based on silica nanoparticles modified with pyrylocyanines exhibited good light resistance. We confirmed that our sensor has high sensitivity for actual use, and 10% solution of butylamine concentration less than 10^{-3} mol/l can be detected. It was shown that the addition of silver nanoparticles into the film of modified silica nanoparticles and the coating it the photonic crystal film as a porous selective mirror on the end of the fiber can increase the sensors sensitivity about 10 times. We assumed that the improving the sensing element by doping it in photonic crystal film with metallic nanoparticles allow us to develop a highly sensitive selective optical chemical sensors remote monitoring.

We found that the position of the stop band in the unchanged spectrum of reflected and refracted Bragg waves for light incident from glass on the interface with the photonic crystal is highly sensitive to a small change in the concentration of vapors of water, ammonia, ethanol or isopropyl alcohol. The observed effect is reversible and can be used to create optical chemical sensors. Thus, the revealed effect of the spectral shift of the stop band of photonic crystals against the chromatic refraction background is well described by the Bragg refraction and the reflection of waves at the glass–photonic crystal interface and can be useful for creating compact, highly sensitive, optical chemical or biological sensors. At the same time, the observed effect of the shift of the stop band of photonic crystals with respect to the unchanged angular spectrum under a small change in the refractive index of the medium filling space between the photonic crystal balls can be used in the schemes of optical sensors, as well as for controlling the spectrum of refracted and reflected light in an optical demultiplexer by an external field. The implementation of the analyzed effect in optical schemes, e.g. with the use of optical fiber technologies, in multiple violated total internal reflection elements, or in intracavity devices, will make it possible to increase the sensitivity of the identification of an element by several orders of magnitude.

6. Acknowledgment

We are grateful to Kalinin D. for placing silica nanoparticle suspensions at our disposal and to Chubakov V. for assistance in the work.

7. References

Baba T. & Nakamura M. (2002). Photonic Crystal Light Deflection Devices Using the Superprism Effect. *IEEE Journal of Quantum Electronics*, Vol. 38, No. 7, pp. 909-914, ISSN 018-9197

Balaban A., Fischer G., Dinulescu A., Koblik A., Dorofeenko G., Mezheritski V. & Schroth W. (1982). Advances in Heterocyclic Chemistry, In: *Pyrylium Salts: Synthesis, Reactions and Physical Properties*, Katritzky A., pp. 429-434, N.-Y. et al. Acad. Press, ISBN 0-12-020652-8

Baldini F., Chester A., Homola J. & Martellucci S. (Eds.). (2006). *Optical Chemical Sensors,* Springer, ISBN 140204609X, Netherlands

Baryshev A., Khanikaev A., Inoue M., Lim P., Sel'kin A., Yushin G. & Limonov M. (2007). Resonant Behavior and Selective Switching of Stop Bands in Three-Dimensional Photonic Crystals With Inhomogeneous Components. *Physics Review Letters*, Vol. 99, No. 6, pp. 063906-1-063906-4

Boldov I., Kuchyanov A., Plekhanov A., Orlova N., Kargapolova I. & Shelkovnikov V. (2011). Fiber-Optic Sensor for Butylamine. *Journal of Physics: Conference Series,* Vol. 291, No. 1, pp. 1-4

Chen L., Kuo C. & Ye Z. (2004). Guiding Optical Flows by Photonic Crystal Slabs Made of Dielectric Cylinders. *Physics Review E*, Vol. 69, No. 6, pp. 066612-1-066612-6

Collinson, M. (2002). Recent Trends in Analytical Applications of Organically Modified Silicate Materials. *Trends in Analytical Chemistry*, Vol. 21, No. 1, pp. 30-38

Foteinopoulou S., Economou E. & Soukoulis C. (2003). Refraction in Media With a Negative Refraction Index. *Physics Review Letters,* Vol. 90, No. 10, pp. 107402-1-107402-4

Geddes C., Cao H., Gryczynski I., Gryczynski Z., Fang J. & Lakowicz J. (2003). Metal-Enhanced Fluorescence Due to Silver Colloids on a Planar Surface: Potential Applications of Indocyanine Green to in Vivo Imaging. *Physical Chemistry,* Vol. 107, No. 18, pp. 3443-3449

Höfelschweiger B. (2005). The Pyrylium Dyes: a New Class of Biolabels. Synthesis, Spectroscopy, and Application as Labels and in General Protein. Assay, *PhD Dissertation*

Janotta M., Katzir A. & Mizaikoff B. (2003). Sol-Gel-Coated Mid-Infrared Fiber-Optic Sensors. *Applied Spectroscopy,* Vol. 57, No. 7, pp. 823-828

Joannopoulos J., Johnson S., Winn J. & Meade R. (2008). *Photonic Crystals: Molding the Flow of Light*, Second Edition, Princeton University Press, ISBN 978-0-691-12456-8, Singapore

Kosaka H., Kawashima T., Tomita A., Notomi M., Tamamura T., Sato T. & Kawakam S. (1998). Superprism Phenomena in Photonic Crystals. *Physics Review B*, Vol. 58, No. 16, pp. 10096-10099

Liang J., Yeh J., Wang C., Liou S., Tsai C. & Chen I. (2002). The New Generation Dihydropyridine Type Calcium Blockers, Bearing 4-Phenyl Oxypropanolamine, Display $_{\alpha}$-/$^{\beta}$-Adrenoceptor Antagonist and Long-Acting Antihypertensive Activities. *Bioorganic & Medicinal Chemistry*, Vol. 10, No. 3, pp. 719-730

Narayanaswamy R. & Wolfbeis O. (Eds.). (2004). *Optical Sensors for Industrial, Environmental and Clinical Applications*, Springer, ISBN 3-540-40888-X, Berlin

Orlova N., Kargapolova I., Shelkovnikov V. & Plekhanov A. (2009). Luminescent Silica Nanoparticles Modified With a Functional Pyrylocyanine Dye. *High Energy Chemistry,* Vol. 43, No. 7, pp. 602–606

Plekhanov A., Kalinin D. & Serdobintseva V. (2006). Nanocrystallization of Single Crystal Opal Films and the Spectral Characteristic of Related Photonic Structures. *Nanotchnologies in Russia,* Vol. 1, No. 1-2, pp. 245-251

Plekhanov A., Kuch'yanov A. & Zabolotskii A. (2009). Features of the Manifestation of a Stop Band in the Spectrum of Light Diffracted at a Glass–Opal Interface. *Journal of Experimental and Theoretical Physics Letters*, Vol. 90, No. 8, pp. 565–568

Sakai Y., Sadaoka Y., Matsuguchi M., Morigaa N. & Shimada M. (1989). Humidity Sensors Based on Organopolysiloxanes Having Hydrophilic Groups. *Sensors and Actuators*, Vol. 16, No. 4, pp. 359-367

Sokolov I., Kievsky Y. & Kaszpurenko J. (2007). Self-Assembly of Ultra-Bright Fluorescent Silica Particles. *Small*, Vol. 3, No. 3, pp. 419-423

Wu L., Mazilu M. & Krauss T. (2003). Beam Steering in Planar-Photonic Crystals: From Superprism to Supercollimator. *Journal of Lightwave Technology,* Vol. 21, No. 2, pp. 561-566, ISSN 0733-8724

Xiao H., Zhang J., Dong J., Luo M., Lee R. & Romero V. (2005). Synthesis of MFI Zeolite Films on Optical Fibers for Detection of Chemical Vapors. *Optics Letters,* Vol. 30, No. 11, pp. 1270-1272

Yakimansky A., Menshikova A., Shevchenko N., Shabsels B., Bazhenova A., Sel'kin A., Sazonov S., Vedernikov A., Gromov S., Sazhnikov V. & Alfimov M. (2009). From Polymeric Nanoparticles to Dye-Containing Photonic Crystals: Synthesis, Self-Assembling, Optical Features, and Possible Applications. *Polymers for Advanced Technologies*, Vol. 20, No. 6, pp. 581-588

Yan H., Wang M., Ge Y. & Yu P. (2009). Colloidal Crystals Self-Assembled on The End Face of Fiber: Fabrication and Characterizations. *Optical Fiber Technology,* Vol. 15, No. 3, pp. 324-327

IntechOpen

IntechOpen

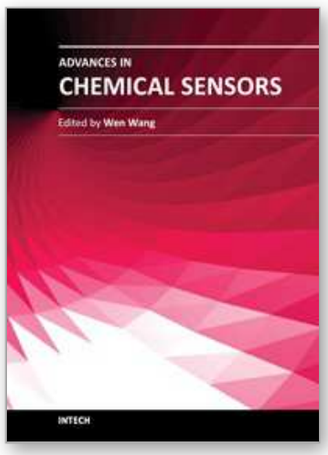

Advances in Chemical Sensors

Edited by Prof. Wen Wang

ISBN 978-953-307-792-5
Hard cover, 358 pages
Publisher InTech
Published online 20, January, 2012
Published in print edition January, 2012

The chemical sensor plays an essential role in the fields of environmental conservation and monitoring, disaster and disease prevention, and industrial analysis. A typical chemical sensor is a device that transforms chemical information in a selective and reversible way, ranging from the concentration of a specific sample component to total composition analysis, into an analytically useful signal. Much research work has been performed to achieve a chemical sensor with such excellent qualities as quick response, low cost, small size, superior sensitivity, good reversibility and selectivity, and excellent detection limit. This book introduces the latest advances on chemical sensors. It consists of 15 chapters composed by the researchers active in the field of chemical sensors, and is divided into 5 sections according to the classification following the principles of signal transducer. This collection of up-to-date information and the latest research progress on chemical sensor will provide valuable references and learning materials for all those working in the field of chemical sensors.

How to reference

In order to correctly reference this scholarly work, feel free to copy and paste the following:

Ivan Boldov, Natalia Orlova, Irina Kargapolova, Alexandr Kuchyanov, Vladimir Shelkovnikov and Alexandr Plekhanov (2012). Optical Sensors Based on Opal Film and Silica Nanoparticles Modified with a Functional Dye, Advances in Chemical Sensors, Prof. Wen Wang (Ed.), ISBN: 978-953-307-792-5, InTech, Available from: http://www.intechopen.com/books/advances-in-chemical-sensors/optical-sensors-based-on-opal-film-and-silica-nanoparticles-modified-with-a-functional-dye

INTECH
open science | open minds

InTech Europe
University Campus STeP Ri
Slavka Krautzeka 83/A
51000 Rijeka, Croatia
Phone: +385 (51) 770 447
Fax: +385 (51) 686 166
www.intechopen.com

InTech China
Unit 405, Office Block, Hotel Equatorial Shanghai
No.65, Yan An Road (West), Shanghai, 200040, China
中国上海市延安西路65号上海国际贵都大饭店办公楼405单元
Phone: +86-21-62489820
Fax: +86-21-62489821

© 2012 The Author(s). Licensee IntechOpen. This is an open access article distributed under the terms of the Creative Commons Attribution 3.0 License, which permits unrestricted use, distribution, and reproduction in any medium, provided the original work is properly cited.

IntechOpen

IntechOpen